# Ozone-induced dissociation of conjugated lipids reveals significant reaction rate enhancements and characteristic odd-electron product ions

**Abstract**

Ozone-induced dissociation (OzID) is an alternative ion activation method that relies on the gas phase ion-molecule reaction between a mass-selected target ion and ozone in an ion trap mass spectrometer. Herein, we evaluated the performance of OzID for both the structural elucidation and selective detection of conjugated carbon-carbon double bond motifs within lipids. The relative reactivity trends for $[M + X]+$ ions (where X = Li, Na, K) formed via electrospray ionization (ESI) of conjugated versus nonconjugated fatty acid methyl esters (FAMEs) were examined using two different OzID-enabled linear ion-trap mass spectrometers. Compared with nonconjugated analogues, FAMEs derived from conjugated linoleic acids were found to react up to 200 times faster and to yield characteristic radical cations. The significantly enhanced reactivity of conjugated isomers means that OzID product ions can be observed without invoking a reaction delay in the experimental sequence (i.e., trapping of ions in the presence of ozone is not required). This possibility has been exploited to undertake neutral-loss scans on a triple quadrupole mass spectrometer targeting characteristic OzID transitions. Such analyses reveal the presence of conjugated double bonds in lipids extracted from selected foodstuffs. Finally, by benchmarking of the absolute ozone concentration inside the ion trap, second order rate constants for the gas phase reactions between unsaturated organic ions and ozone were obtained. These results demonstrate a significant influence of the adducting metal on reaction rate constants in the fashion Li > Na > K.

**Keywords**

dissociation, induced, ozone, electron, odd, characteristic, enhancements, rate, reaction, significant, ions, reveals, product, lipids, conjugated

**Disciplines**

Medicine and Health Sciences | Social and Behavioral Sciences

**Publication Details**

Pham, H. T., Maccarone, A. T., Campbell, J. Larry., Mitchell, T. W. & Blanksby, S. J. (2013). Ozone-induced dissociation of conjugated lipids reveals significant reaction rate enhancements and characteristic odd-electron product ions. Journal of the American Society for Mass Spectrometry, 24 (2), 286-296.

# Ozone-Induced Dissociation of Conjugated Lipids Reveals Significant Reaction Rate Enhancements and Characteristic Odd-electron Product Ions

Huong T. Pham[1], Alan T. Maccarone[1], J. Larry Campbell[2], Todd W. Mitchell[3], Stephen J. Blanksby[1]*

[1] School of Chemistry, University of Wollongong, Australia

[2] AB SCIEX, Concord, ON, Canada

[3] School of Health Sciences, University of Wollongong, Australia

* Author to whom correspondence should be addressed

Address reprint request to:
Dr. Stephen J. Blanksby
School of Chemistry, University of Wollongong
Northfields Rd., Wollongong, NSW 2522, Australia.
Email: blanksby@uow.edu.au

**ABSTRACT**

Ozone-induced dissociation (OzID) is an alternative ion activation method that relies on the gas phase ion-molecule reaction between a mass-selected target ion and ozone in an ion trap mass spectrometer. Herein, we evaluated the performance of OzID for both the structural elucidation and selective detection of conjugated carbon-carbon double bond motifs within lipids. The relative reactivity trends for $[M+X]^+$ ions (where X = Li, Na, K) formed via electrospray ionization (ESI) of conjugated versus non-conjugated fatty acid methyl esters (FAMEs) were examined using two different OzID-enabled linear ion-trap mass spectrometers. When compared with non-conjugated analogues, FAMEs derived from conjugated linoleic acids were found to react up to 200 times faster and to yield characteristic radical cations. The significantly enhanced reactivity of conjugated isomers means that OzID product ions can be observed without invoking a reaction delay in the experimental sequence (*i.e.*, trapping of ions in the presence of ozone is not required). This possibility has been exploited to undertake neutral-loss scans on a triple quadrupole mass spectrometer targeting characteristic OzID transitions. Such analyses reveal the presence of conjugated double bonds in lipids extracted from selected foodstuffs. Finally, by benchmarking of the absolute ozone concentration inside the ion trap, second order rate constants for the gas phase reactions between unsaturated organic ions and ozone were obtained. These results demonstrate a significant influence of the adducting metal on reaction rate constants in the fashion Li > Na > K.

## INTRODUCTION

While unsaturated lipids containing conjugated carbon-carbon double bonds are less common in nature than non-conjugated variants [1], they are known to profoundly influence the physiology of plants and animals [2-4]. One of the better known classes of conjugated lipids is conjugated linoleic acids (CLA). These octadecadienoic acids (18:2) possess two carbon-carbon double bonds in conjugation and give rise to variation from the differing positions and stereochemistry of these bonds. CLAs are reported to have a number of beneficial properties, such as inhibiting cancer growth and reducing obesity rates [5, 6], and as a result, their dietary intake has become a subject of some interest. The richest naturally occurring dietary sources of CLAs are from ruminant animals, most notably beef and dairy products [7, 8]. In the case of organic beef, the non-conjugated isomers are reported to be approximately 25 times more abundant than certain CLA isomers [1]. Synthetic CLAs have also emerged as common dietary supplements and are manufactured from non-conjugated linoleic acids [9, 10] – present at high abundance in common vegetable oils, such as soybean and safflower – by iodine catalyzed UV photoisomerization [11].

Importantly, the biological functionality of CLAs has been demonstrated to be isomer specific. Prior work on the effects of CLAs suggests that each isomer has distinct impacts on adipogenesis and lipid metabolism [12-15] as well as the inhibition of some cancers [16] and atherosclerosis [17, 18]. Such divergent physiological properties of these isomeric fatty acids is perhaps not surprising given the differences in molecular structure brought about by the position and stereochemistry of the double bonds. Indeed, the difference in geometrical and positional arrangements of the conjugated double-bond system has been implicated in the preferential oxidation of 18:2(10*E*,12*Z*) in mitochondria, leading to preferential tissue accumulation of the 18:2(9*Z*,11*E*) isomer [19, 20]. Such observations are part of a broader picture, where seemingly minor disturbances in lipids at the molecular level (for instance, double-bond location) are associated with changes in metabolism and disease [21-23].

Owing to these important findings, there is a need for further examination of the amount and isomer-specific makeup of CLAs in natural and synthetic sources. Such analyses present some significant challenges in: (i) the unambiguous identification of lipids, in particular the characterization of distinct isomers differing only in double-bond position and/or stereochemistry and (ii) the detection and ultimately the quantification of low abundant - but nonetheless bioactive - lipids in the presence of more ubiquitous isomeric variants. To address these challenges, fatty acyl components are typically liberated from complex lipids by hydrolysis, derivatized to fatty acid methyl esters (FAMEs) and subjected to separation by gas chromatography (GC) or high performance liquid chromatography (HPLC). Such chromatographic approaches provide effective separation of fatty acid isomers, including double-bond positional and geometric isomers [24, 25]. Unfortunately, the identification of specific isomers requires comparison of retention times with standard reference compounds that may not be commercially available [26]. Alternatively, an offline chemical derivatization of the conjugated diene itself can facilitate the assignment of double-bond location in unsaturated lipids. This can include solution-based methods (e.g., using Diels-Alder reactions [27]) or even gas-phase derivatizations. An example of the latter is covalent adduct chemical ionization tandem mass spectrometry (CACI-MS/MS) [28]. In CACI-MS/MS, gas-phase ion-molecule reactions between unsaturated lipids and a selective reagent ion produce adducts in the chemical ionization (or atmospheric pressure chemical ionization) source of the mass spectrometer. Subsequent collision-induced dissociation (CID) of these adducts gives diagnostic and predictable product ions that can be used to localize double bond position(s). This approach has been combined with chromatography to effect the separation and identification of polyunsaturated FAMEs derived from a range of isomeric linoleic and linolenic acids [29]. Intriguingly, Brenna and co-workers found distinctive behavior for FAMEs bearing conjugated dienes, noting that the appearance of diagnostic $\alpha$-and $\omega$-product ions strongly depended on the geometry (*i.e.*, *cis* and *trans*) of the double bonds [29].

Ozone-induced dissociation (OzID) is another technique that takes advantage of selective gas-phase ion-activation for the characterization of unsaturated lipid isomers. OzID utilizes the chemically selective reaction between ozone and carbon-carbon double bonds to identify both the degree and position(s) of unsaturation in individual, intact lipid ions inside the mass spectrometer [30]. While CACI-MS/MS relies on an in-source chemical modification of lipid molecules prior to any mass selection, OzID begins with the conventional electrospray ionization (ESI) of lipids that are then mass-selected before undergoing ion-molecule reactions with ozone. This technique has been used to identify isomeric lipids differing in double-bond position from complex biological extracts, including olive oil [30], human lens [31], and cow brain [32]. Here, we demonstrate, for the first time, the effectiveness of OzID analysis on conjugated lipids and report a remarkable enhancement in the rate of the ion-molecule reaction in the presence of this bonding motif. In addition, when FAMEs of conjugated linoleic acids are ionized and allowed to react with ozone inside an ion trap mass spectrometer, distinctive odd-electron product ions are observed that are diagnostic for the presence and position of the conjugation in the lipid. This combination of fast reaction rates and characteristic OzID ions allows for the facile detection and identification of CLAs in foodstuffs without prior fractionation despite the presence of abundant non-conjugated variants.

## EXPERIMENTAL

*Materials*

Four isomers of linoleic acid (18:2) methyl ester were purchased from Nu-Chek Prep (Elysian, Minnesota, USA): (9*Z*,11*E*), (10*E*,12*Z*), (9*Z*,12*Z*) and (9*E*,12*E*). Potassium acetate, sodium acetate, lithium acetate, and a 10% solution of boron trifluoride in methanol were purchased from Sigma-Aldrich (Castle Hill, NSW, Australia). All solvents (HPLC grade) were purchased from Ajax Finechem (Sydney, NSW, Australia) and were used without further purification. Extra virgin safflower oil was purchased from Proteco (Kingaroy, Queensland, Australia) and CLA dietary supplements (NOW Foods, Bloomingdale, Illinois, USA) were purchased from a local healthfood store. The supplement packaging indicates that each 800 mg capsule contains 740 mg of CLAs including both the (9*Z*,11*E*) and (10*E*,12*Z*) isomers. Where the position and stereochemistry of the double bonds within a lipid are both defined, we adopt the recommended nomenclature (*e.g.*, (9*Z*,11*E*)) in which positions of unsaturation are indicated by the number of carbon-carbon bonds from the carboxylate moiety, and *Z* (*cis)* and *E* (*trans)* indicate the stereochemistry [33, 34]. However, in some instances, we employ the traditional nomenclature "*n*-x" where "*n*" refers to the number of carbon atoms in the chain and subtracting "x" provides the location of the double bond [35]; for example, 18:2(9*Z*,11*E*) becomes 18:2(*n*-9,*n*-7), noting that the latter does not define the stereochemistry. This nomenclature is instructive for OzID analysis as the observed neutral losses are common to all lipids with double bonds in the same position relative to the highest numbered carbon on the alkyl chain.

Solutions of the four FAME standards were prepared in methanol at concentrations of 20 μM, followed by addition of potassium, sodium, or lithium acetate (in methanol) to yield a final alkali metal ion concentration of 50 μM. These dopants aid in the formation of metal-adducted ions during ESI. Approximately 20 mg of each of the safflower oil and the CLA dietary supplements were dissolved in 1 mL of a 10% $BF_3$ in methanol solution at room temperature and stirred for 20 minutes. Water (0.5 mL) and pentane (1 mL) were then sequentially added to the solution, followed by separation of the organic layer that contained the extracted FAMEs at a

concentration of *ca*. 70 mM. This solution was diluted to 35 μM with methanol before doping with the appropriate alkali metal salt.

*Instrumentation*

Two OzID-equipped mass spectrometers were employed to analyze the lipid samples. One is a modified Thermo Fisher Scientific LTQ single stage linear ion-trap mass spectrometer (San Jose, CA, USA). Modifications to allow the observation of ion-molecule reactions, including OzID, have been described in detail previously [30]. Sample solutions were directly infused and ionized *via* the ESI source with conditions as follows: the sample flow rate was 5 μL/min, the source voltage was set at 4 kV, the tube lens voltage was set to 78 V and the capillary voltage at 21 V. The heated capillary temperature was maintained at 200 °C and nitrogen served as the sheath, auxiliary and sweep gases. Ozone was generated by an offline HC-30 ozone generator (Ozone Solutions, Sioux Center, Iowa, USA) and was collected in a 10 mL disposable, ozone-resistant plastic syringe (Livingstone). Ozone was introduced by attaching the syringe to a PEEKsil tubing restrictor (100 mm L x 1/16" OD x 0.025 mm ID, SGE) connected to the helium supply line downstream of the metering flow valve. Backing pressure was applied to the syringe using a syringe pump set to 25 μL/min. Instrument modifications by-pass the helium splitter and the helium flow rate was manually adjusted using a metering flow valve (Granville-Phillips) so that the ion gauge pressure read approximately $0.8 \times 10^{-5}$ Torr corresponding to an estimated total pressure of 2.5 mTorr within the ion trap. OzID spectra were acquired with the collision energy set to zero, the isolation width set between 2 and 5 Da, and activation times between 0.01 and 10 s. $MS^3$ experiments were performed whereby OzID product ions were re-isolated and subjected to collision-induced dissociation (OzID/CID) or further OzID (OzID/OzID). In the former case, the normalized collision energy was set to 22 (arbitrary units). All spectra presented here are averages of at least 50-100 scans.

The second instrument employed was an AB SCIEX QTRAP2000 tandem linear ion-trap mass spectrometer (Concord, ON, Canada) that has been previously modified to incorporate

ozone generated online by a model Atlas ozone generator (Absolute Ozone, Alberta, Canada) [32]. Ions were generated by direct infusion ESI with nitrogen as the nebulizing gas, and optimized source parameters as follows: the ionspray voltage was set to 4.5 kV; the declustering potential was 60 V; and the entrance potential was 10 V. Typical OzID experimental conditions had the oxygen flow rate through the generator set to 250 mL/min with the ozone generator power output at 40% to obtain approximately 180 g $N/m^3$ of ozone (8.4% v/v) as measured immediately downstream of the generator using a Mini-HiCon ozone monitor (IN USA, Norwood, MA, USA). The gas flow from the generator was split with the majority passed through an ozone destruct catalyst (IN USA, Norwood, MA, USA). High-concentration ozone (in oxygen), controlled by a variable leak valve (VSE Vacuum Technology, Lustenau, Austria), was mixed with the collision gas (nitrogen) supply prior to entering q2. OzID spectra were acquired by first mass-selecting precursor ions using Q1, which were subsequently injected into q2 (collision energy set to 12 eV). Ions were accumulated in q2 for 50 ms after which time these ions were trapped in q2 for varying reaction times (0.01 to 10 s). Product ions were then transferred to the linear ion trap (Q3) and cooled prior to mass analysis. Neutral loss mass spectra were obtained using the same ozone conditions described above. Default neutral loss settings provided by the Analyst control software (Version 1.5, AB SCIEX) were employed for this experiment with a collision energy of 15 eV. All spectra are reported as an average of 50-100 scans.

## RESULTS & DISCUSSION

*Ozone induced dissociation of conjugated FAMEs*

One of the initial findings of this study was the apparent enhancement of OzID reaction rates for conjugated FAMEs over a non-conjugated analogue. For example, Figure 1 shows OzID spectra acquired for the sodium adduct ions formed from representative conjugated and non-conjugated FAME isomers on the single-stage LTQ mass spectrometer. The $[M+Na]^+$ precursor ions can be observed at *m/z* 317 for all three isomers along with distinctive product ions in each case. Given that all three spectra were acquired under identical conditions, a striking feature emerges with the high abundances of OzID products ions present in Figures 1(a) and (b) relative to those in Figure 1(c). This suggests that the reaction of the conjugated isomers with ozone is substantially faster, with approximately 50% of the precursor ions converted to ozonolysis products within a reaction time of only 0.5 s. In contrast, the non-conjugated FAME (18:2(9*Z*,12*Z*)) displays *ca*. 5% conversion even after a 10-s reaction time, which is similar in efficiency to previous observations of OzID on monounsaturated lipids [30]. These qualitative trends suggest dramatic enhancements in reaction efficiency for conjugated over non-conjugated species that are quantified in a later section of this paper.

The spectrum obtained from FAME (18:2(9*Z*,11*E*)) (Figure 1a) reveals product ions at *m/z* 235 and 209 that are assigned as the aldehydes expected from oxidative cleavage of the *n*-7 (-82 Da) and *n*-9 (-108 Da) double bonds, respectively. These assignments are based on a mechanistic understanding of the reaction of ozone with olefins and can be used to predict neutral losses arising from different double-bond positions in any unsaturated lipid [36]. This reaction pathway is depicted for the [FAME (18:2(9*Z*,11*E*))+Na]$^+$ cation in Scheme I(a). By extension, neutral losses of 68 and 94 Da are predicted to occur during OzID of the alternative conjugated isomer FAME (18:2(10*E*,12*Z*)); indeed, the corresponding ions are observed at *m/z* 249 and 223 in Figure 1(b). The presence of the *m/z* 235 product ion – nominally diagnostic of the double bond at the *n*-7 position – in the OzID spectrum of FAME (18:2(10*E*,12*Z*)) is unexpected. Independent GC analysis (see Supporting Information, Figure S1), confirms the

presence of a trace amount of FAME (18:2(9*Z*,11*E*)) in this sample. Hence, this feature is assigned as arising from ozonolysis of this contaminant (*cf*. *m/z* 235 in Figure 1a). For the non-conjugated FAME (18:2(9*Z*,12*Z*)), product ions are found at *m/z* 249 and 209 and match the neutral losses of 68 and 108 Da, respectively, arising from oxidation at the expected double-bond positions. Overall, OzID of each of the three linoleic acid isomers yields not only distinctive spectra but, importantly, product ions indicative of double-bond position, allowing unambiguous identification in each case. More significantly, these data demonstrate that the central capability of OzID (*i.e.*, to assign double-bond position) is unaffected by the presence of conjugated double-bond motifs and may even enhance the analysis of this class of lipid (*see below*).

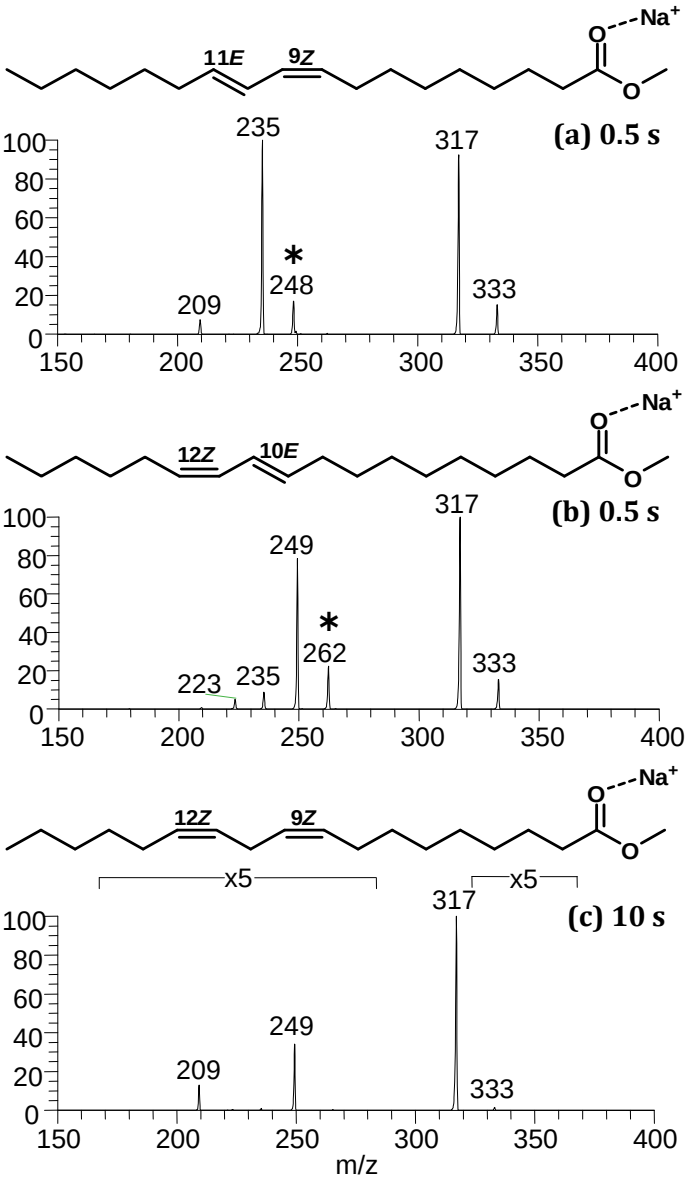


**Figure 1** OzID spectra acquired for sodium adducts of three FAME (18:2) isomers (a) conjugated [FAME (18:2(9*Z*,11*E*))+Na]$^+$ for a 0.5 s reaction time, (b) conjugated [FAME (18:2(10*E*,12*Z*))+Na]$^+$ for a 0.5 s reaction time and (c) non-conjugated [FAME (18:2(9*Z*,12*Z*))+Na]$^+$ for a 10 s reaction time. [M+Na]$^+$ precursor ions appear at *m/z* 317 in all three spectra, as well as an [M+Na+16]$^+$ ion at *m/z* 333. Peaks with an even *m/z* correspond to radical cations formed from conjugated FAMEs and are marked with an asterisk (∗)

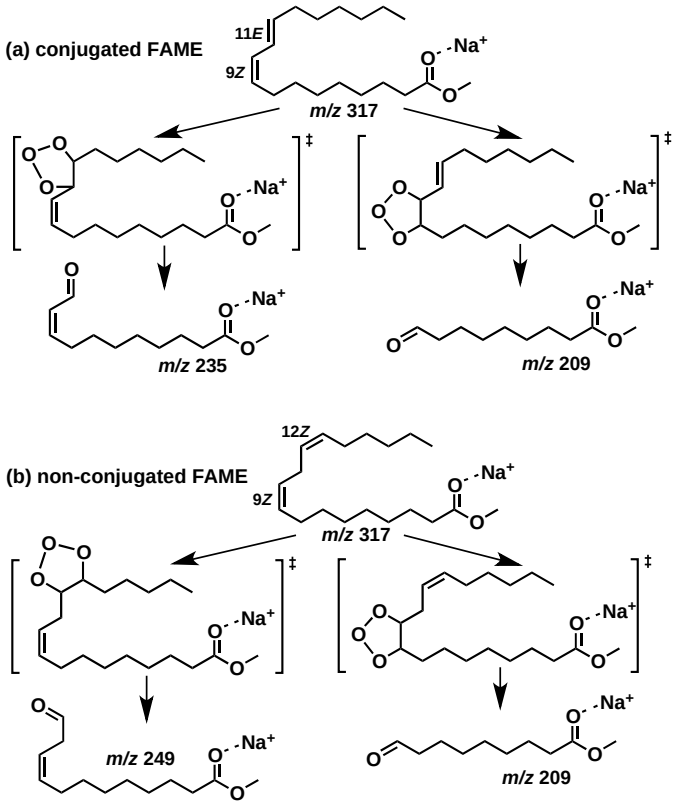


**Scheme I** Proposed reaction pathways for OzID on the sodium adducts of (a) the conjugated FAME (18:2(9*Z*,11*E*)) and (b) the non-conjugated FAME (18:2(9*Z*,12*Z*)). The two aldehyde product ions in each case can be used to locate the positions of unsaturation for each isomer unambiguously

Although aldehyde product ions are observed from oxidation of each double bond for three FAME isomers, the corresponding Criegee ions are notably absent from the spectra in Figure 1. These ions would be expected to appear 16 Da above the corresponding aldehyde and have been consistently observed in OzID analyses of a structurally diverse array of unsaturated lipids [30, 32]. The absence of Criegee ions for cationized FAMEs does not diminish the structure elucidation ability of OzID: the aldehyde ions alone can be used for the assignment of double-bond position. However, this subtle difference between OzID spectra of $[FAME+Na]^+$ ions and those of other unsaturated lipids - including the $[M–H+2Na]^+$ ions of analogous free fatty acids - is evidence of different product branching ratios in the ozonolysis reaction. In particular, it highlights the influence of both the number and type of metal ion(s) and the nature and position of other functional groups present in the lipid (e.g., carboxylic acid versus methyl ester moieties), in influencing the product ion distribution. In other words, the depiction of ozonolysis occurring at a remote double bond and uninfluenced by the headgroup and the charge (*cf.* Scheme I) is an oversimplification and the three-dimensional gas-phase structure of the ionized lipid is likely critical in controlling product branching ratio and reaction rate (*see below*).

*Characterization of odd-electron product ions*

Another striking difference between the OzID spectra of the conjugated FAMEs and the non-conjugated isomer is the appearance of an unusual product ion of even *m/z* that is exclusive to the conjugated species. For example, ozonolysis of [FAME (18:2(9*Z*,11*E*))+Na]$^+$ gives rise to the prominent peak at *m/z* 248, corresponding to a neutral loss of 69 Da from the precursor ion (marked with an asterisk (*) in Figure 1a). Similarly, a peak at *m/z* 262 is observed in the spectrum of the FAME (18:2(10*E*,12*Z*)) (marked with an asterisk (*) in Figure 1b), representing a 55 Da neutral loss. These even-*m/z* product ions could be rationalized as either: (i) radical ions containing sodium or (ii) even-electron species arising from neutral loss of the metal. In order to determine which was the case, OzID was performed on both the potassium and lithium

adduct ions of the same suite of FAME isomers. The $[M+K]^+$ spectra are shown in Figure 2 while the analogous $[M+Li]^+$ data are provided as Supporting Information (Figure S2). As expected, the previously assigned aldehyde ions, arising from ozonolysis at each double bond, are also observed in Figure 2 where they are shifted up by 16 Da from their counterparts in Figure 1, consistent with the mass difference between sodium and potassium. Importantly, the potassiated ions also undergo neutral losses of 69 and 55 Da from [FAME (18:2(9*Z*,11*E*))+K]$^+$ and [FAME (18:2(10*E*,12*Z*))+K]$^+$, respectively (marked with an asterisk (*) in Figure 2). The analogous neutral losses are also observed for the lithiated species (Figure S2). These data demonstrate that the even-*m/z* product ions observed for conjugated FAMEs include the adducting metal and thus represent a characteristic odd-electron species arising from the ozonolysis reaction. This conclusion is supported by the $MS^3$ spectra shown in Figure 3 that were acquired by subjecting mass-selected OzID product ions (*i.e.*, *m/z* 248 and 262 ions from OzID of [FAME (18:2(9*Z*,11*E*))+Na]$^+$ and [FAME (18:2(10*E*,12*Z*))+Na]$^+$, respectively) to further interrogation by CID on the single-stage LTQ. The resulting OzID/CID mass spectra reveal extensive fragmentation along the hydrocarbon chain reminiscent of the dissociation of radical cations observed following electron ionization (EI) [37], or EI-CID mass spectrometry [38].

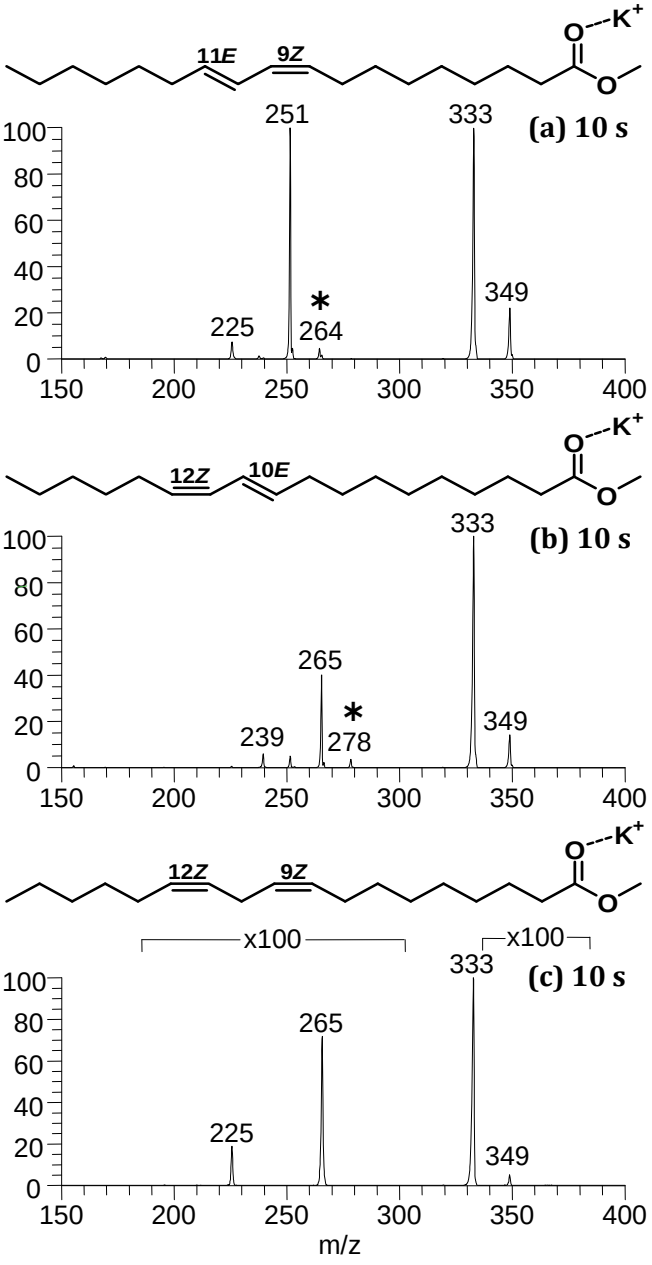


**Figure 2** OzID spectra acquired with a 10 s reaction time in each case for potassium adducts of the FAME (18:2) isomer precursor ions at *m/z* 333: (a) conjugated [FAME (18:2(9*Z*,11*E*))+K]$^+$, (b) conjugated [FAME (18:2(10*E*,12*Z*))+K]$^+$ and (c) non-conjugated [FAME (18:2(9*Z*,12*Z*))+K]$^+$. Peaks with an even mass correspond to radical cations formed from conjugated FAMEs and are marked with an asterisk (∗)

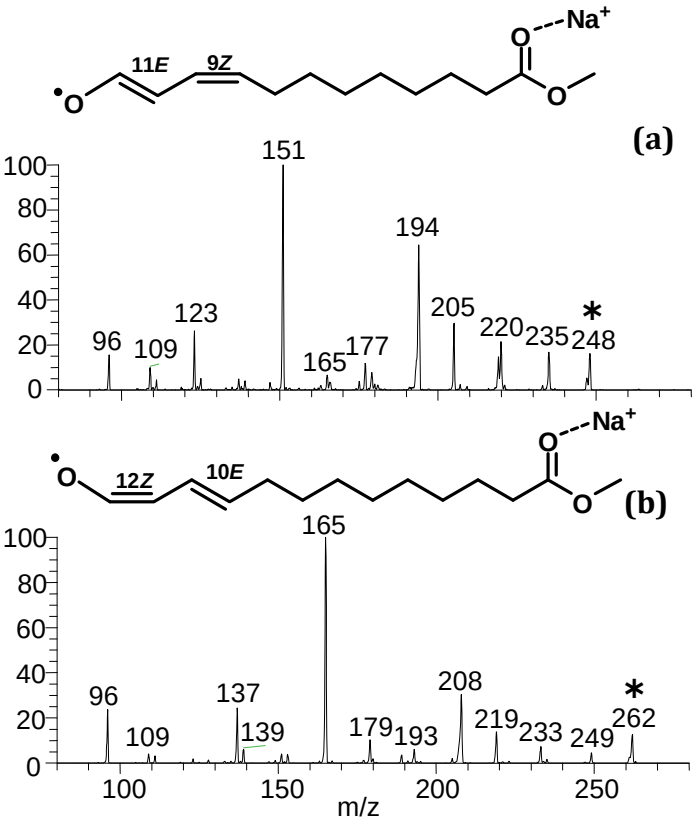


**Figure 3** OzID/CID spectra obtained by performing CID on the even-mass OzID ions derived from the conjugated isomers (a) [FAME(18:2 (9*Z*,11*E*))+Na]$^+$ and (b) [FAME(18:2 (10*E*,12*Z*))+Na]$^+$. The proposed structures of the radical cations at *m/z* 248 and 262 ions are drawn above each spectrum

Potential reaction pathways resulting in odd-electron products from the gas-phase ozonolysis of conjugated FAMEs are illustrated in Scheme II. While the first step in this process remains the formation of a primary ozonide, we propose that, in the case of conjugated double bonds, competition exists in the pathways for dissociation of this reactive intermediate. That is, dissociation can either proceed *via* the classical Criegee pathway (*cf*. Scheme I) or with loss of dioxygen and a hydrocarbon radical. This mechanism is illustrated for [FAME (18:2(9*Z*,11*E*))+Na]$^+$ in Scheme II where dissociation of the primary ozonide at the *n*-7 double bond can lead to formation of the radical ion at *m/z* 248 by loss of dioxygen and the $^{\bullet}C_6H_{13}$ radical in either a step-wise or concerted fashion. Formation of dioxygen in any rearrangement clearly provides a strong thermodynamic driver and additional evidence for its participation is provided by the observation of *m/z* 333 and 349 ions in the OzID spectra in Figures 1 and 2, respectively. Scheme II indicates that ejection of dioxygen, alone or coupled with the loss of the hydrocarbon radical, gives rise to resonance-stabilized radicals and thus accounts for: (i) the exclusive observation of the radical ion products for conjugated FAME isomers and (ii) a much greater abundance of the *m/z* 333 product ion for the conjugated than non-conjugated isomers (see Figures 1 and 2). The significant resonance stabilization of the radical ion arising from dissociation of the *n*-7 ozonide (with a conjugated $\pi$-network that can be represented as a hybrid of up to three allylic resonance forms [39]) also accounts for the absence of an abundant ion arising from the analogous dissociation of an *n*-9 ozonide. Production of carbon-centered radicals in the ozonolysis of alkenes, as illustrated in Scheme II, has some precedent in condensed-phase chemistry where, for example, *tert*-butyl radicals were detected from the ozonolysis of *tert*-butyl substituted ethylene accounting for 10% of the reaction flux [40].

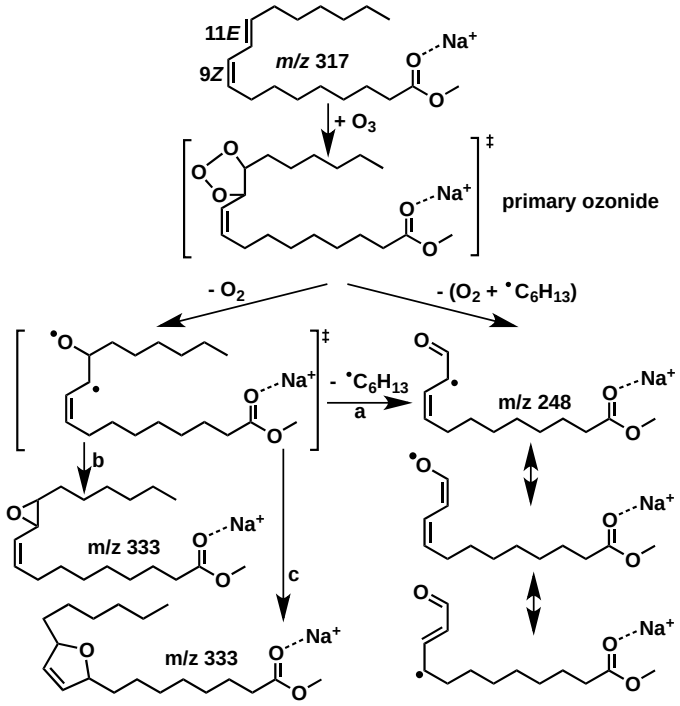


**Scheme II** Proposed mechanism for the formation of the radical cation (*m/z* 248) upon OzID of the conjugated [FAME (18:2(9*Z*,11*E*))+Na]$^+$

Scheme II depicts two potential structures for product ions arising from neutral loss of dioxygen from the activated ozonide that could account for the feature seen at *m/z* 333 in all three spectra in Figure 1. In order to probe the structure of these product ions, experiments were conducted for both of the conjugated [FAME (18:2)+Na]$^+$ precursor ions where *m/z* 333 product ions were mass-selected and subsequently allowed to react further with ozone. The resulting OzID/OzID mass spectra are shown in Figure 4 and display two important features. First, further oxidative cleavage of the chain is achieved, thus supporting the proposed oxirane structure over the dihydrofuran-based alternative. The second feature reveals the presence of two ozone-derived aldehydes (*e.g., m/z* 251 and 209 from [FAME (18:2(9*Z*,11*E*))+Na+O]$^+$ in Figure 4a), thus indicating that epoxides are formed at both *n*-7 and *n*-9 double bond positions (see inset to Figure 4). Interestingly, the abundance of the ozonolysis products arising from both [FAME+Na+16]$^+$ species (Figure 4) is remarkably low relative to those from the corresponding [FAME+Na]$^+$ precursor ions (Figure 1), in spite of the much greater (10 s) reaction time employed for the former case. This comparison stands as an additional illustration of the influence of double-bond conjugation on reaction rate where removing one of the two double bonds from the conjugated motif (by blocking with oxygen) drastically reduces the rate of ozonolysis at the remaining site of unsaturation. OzID/OzID analysis of lithium adduct ions of the same FAME (18:2) isomers produces a qualitatively similar decrease in reaction rate (Supporting Information Figure S3).

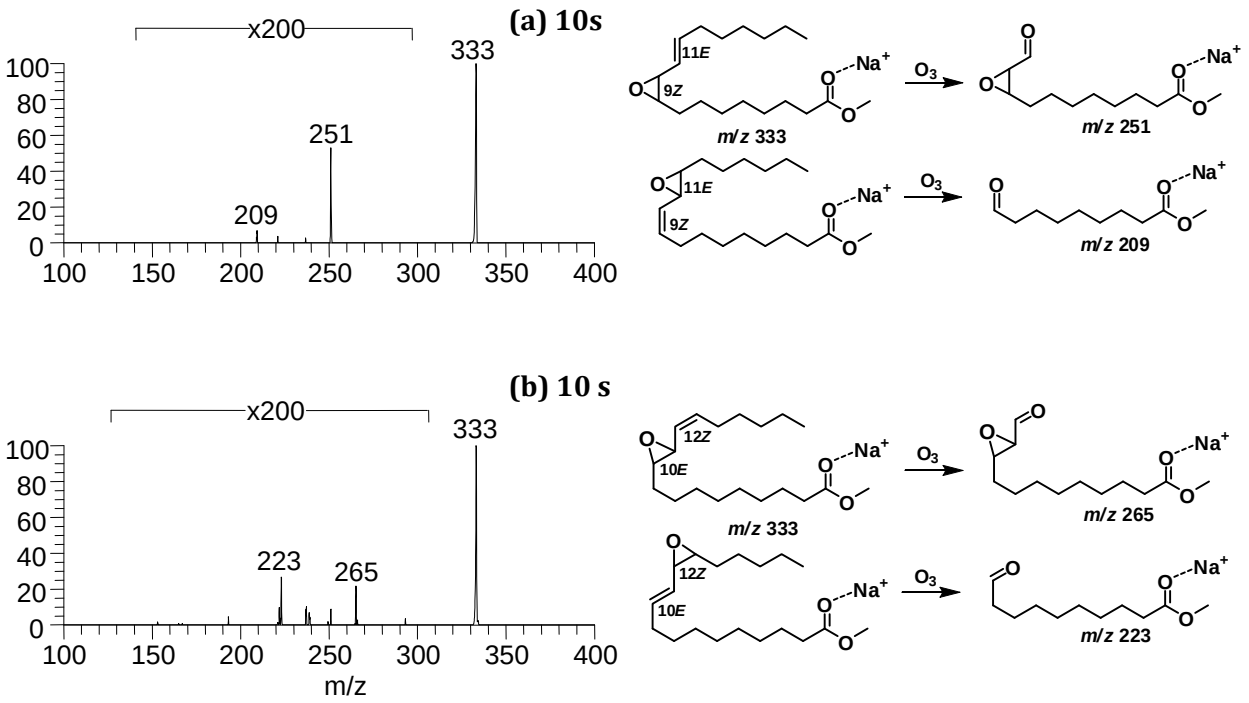


**Figure 4** OzID/OzID spectra acquired with a 10 s reaction time in each case for the $[M+Na+16]^+$ ions derived from OzID of the two conjugated FAME (18:2) isomers (a) FAME (18:2(9*Z*,11*E*)) and (b) FAME (18:2(10*E*,12*Z*)). The two major product ions marked in each spectrum can be rationalized as aldehydes formed from the OzID of the putative epoxide structures shown

*Measurement of reaction kinetics*

The qualitative analysis discussed above points to a significantly greater OzID reactivity of conjugated FAMEs compared to non-conjugated cases. In order to quantify this, OzID of the metal-adducted FAME standards was conducted using a modified tandem linear ion-trap mass spectrometer (QTRAP). The online generation of ozone previously engineered on this instrument provides stable and reproducible ozone concentrations allowing for reliable pseudo-first-order kinetic measurements to be conducted [32]. Plots showing the change in [FAME (18:2)+X]$^+$ (where X = Li, Na, K) precursor ion signal as a function of reaction time are provided as Supporting Information (Figure S4) and first-order rate constants calculated from these data are compiled in Table 1. Comparing the kinetics of [M+Na]$^+$ ions formed from FAME (18:1(9*Z*,11*E*)) and FAME (18:2(9*Z*,12*Z*)) shows a remarkable 220-fold increase in rate constant in favor of the conjugated isomer. Similar trends were observed for potassiated ions (*i.e.*, 80-fold increase) while the lithiated analogues of the two conjugated FAMEs reacted too swiftly for reliable measurement of the reaction rate constant. Even when compared to FAME (18:2(9*E*,12*E*)) - the faster reacting of the two non-conjugated isomers - the slowest conjugated FAMEs returns a rate constant some 25-times greater for a given metal adduct. Previously measured ozonolysis rate constants for neutral dienes also show a kinetic advantage for conjugated over non-conjugated analogues, but the magnitude of the enhancement is only modest. For example, the rate constant merely doubles when comparing non-conjugated 1,4-pentadiene with conjugated 1,3-pentadiene [41, 42]. This comparison also suggests that the adducting metal ion influences the ozonolysis reaction perhaps *via* chelation of the double bond(s). The data in Table 1 also quantify the impact of double-bond geometry on ozonolysis reaction rates and are consistent with qualitative trends previously reported for OzID on stereoisomeric phospholipids and fatty acids [32]. For example, the all *trans* isomer FAME (18:2(9*E*,12*E*)), reacts *ca*. 1.5 times faster than its *cis* counterpart, FAME (18:2(9*Z*,12*Z*)), for a given metal adduct.

**Table 1** Rate constants measured on a tandem linear ion-trap mass spectrometer (QTRAP) for the gas-phase ozonolysis reactions of metal adducted FAME standards. Pseudo-first-order values, $k^{I}$, were calculated from raw kinetics data provided as Supporting Information (Figure S4). The absolute second order rate constants, $k^{II}$, are calculated by benchmarking to the known $k^{II}$ for the gas-phase reaction $I^- + O_3 \rightarrow IO_3^-$ [46]. Reaction efficiencies ($\Phi$) are presented in square brackets as a percentage of the calculated collision rate.

| | $k^{I} = k^{II}[O_3]$ $(s^{-1})$[f] | | | | $k^{II}$ $(x10^{-12}$ $cm^3$ $molecules^{-1}$ $s^{-1})$ $[\Phi\ \%]$[a] | |
|---|---|---|---|---|---|---|
| Metal adduct **FAME (18:2)** | $K^+$ | $Na^+$ | $Li^+$ | | $K^+$ | $Na^+$ | $Li^+$ |
| **(9*Z*,11*E*)** | 3.20 ± 0.02 | 1.30 ± 0.05[e] | -[d] | | 4 ± 1 [0.5] | 110 ± 30 [14][e] | -[d] |
| **(10*E*,12*Z*)** | 1.60 ± 0.02 | 17.6 ± 0.3 | -[d] | | 2.1 ± 0.5 [0.3] | 23 ± 6 [3] | -[d] |
| **(9*Z*,12*Z*)** | 0.0411 ± 0.0006 | 0.357 ± 0.003 | 5.50 ± 0.03 | | 0.05 ± 0.01 [0.01] | 0.5 ± 0.1 [0.1] | 7 ± 2 [0.9] |
| **(9*E*,12*E*)** | 0.064 ± 0.001 | 0.503 ± 0.003 | 7.7 ± 0.1 | | 0.08 ± 0.02 [0.01] | 0.6 ± 0.2 [0.1] | 10 ± 2 [1] |
| $I^-$ | 7.8 ± 0.1[b] | | | | 10 ± 3[c] | | |

a. Reaction efficiencies based on theoretical collision rates calculated from a parameterized trajectory model [47].
b. $I^-$ was run before and after all FAME experiments were conducted to monitor ozone concentration.
c. Reference [46].
d. Reactions were too fast for reliable measurements under these experimental conditions.
e. [FAME(18:2 (9*Z*,11*E*))+Na]$^+$ was run on a separate day under ozone conditions which yielded $k^{I}(I^-) = 0.122 \pm 0.003\ s^{-1}$.
f. Errors in $k^{I}$ values represent the standard error in the slope of a line fit to the data (see Supporting Information Figure S4); errors in $k^{II}$ values represent a least squares analysis using the $k^{I}$ errors and the absolute errors of ± 25% quoted by Williams *et al.* [46].

In the absence of conjugation, this result shows good agreement with established trends in the gas-phase ozonozlysis of alkenes where *trans* olefins react *ca*. 1.4 times faster than their *cis* counterparts [43].

The data in Table 1 demonstrate how changing the alkali metal adducted to a given FAME (18:2) isomer impacts the rate of ozonolysis. The rate constant is seen to decrease with increasing metal ion radius (*i.e.,* $Li^+ > Na^+ > K^+$). Trends in binding energy of alkali metals with common ligands have been tabulated from guided ion beam studies [44], and it is understood that binding energy decreases gradually from $Li^+$ to $Cs^+$ for a given organic ligand. This is explained by an increase in the metal ion radius causing a longer bond length, and hence, weakening of the electrostatic interaction. Recent *ab initio* calculations compute a decrease in [M-ethylene]$^+$ gas-phase binding energies with increasing ionic radius of M (19.4 kcal mol$^{-1}$ for $Li^+$, 12.0 kcal mol$^{-1}$ for $Na^+$, and 8.0 kcal mol$^{-1}$ for $K^+$) [45]. This trend is consistent with the OzID reactivity trend observed here and supports the proposal of a direct interaction of the metal with the site of unsaturation. This suggests that the increased interaction energy is, in part, responsible for lowering the activation barrier to reaction with ozone.

While the concentration of ozone being generated was measured external to the mass spectrometer, the number density of ozone inside q2 could not be directly measured in our configuration. Fortunately, the second order rate constant for the reaction of the iodide anion with ozone has previously been reported based on selected-ion flow tube measurements ($k^{II}[I^- + O_3] = 1 \times 10^{-11}$ cm$^3$ molecules$^{-1}$ s$^{-1}$ [46]). Thus, measuring the pseudo-first order rate constant for this reaction on our instrument was used along with the reported second-order rate constant to benchmark the ozone concentration in q2. Hence, we have obtained $k^{II}$ values for the OzID reactions of the metal adducted FAMEs studied herein. These results are reported in Table 1 and are the first such rate constants reported for the reactions of organic ions with ozone in the gas phase. Importantly, by comparison with calculated collision rates [47], it is now possible to derive the absolute reaction efficiencies: these range from 0.01% for the potassium adducts of non-conjugated FAME (18:2) up to 14% for sodium adducts of conjugated forms. The reaction

efficiencies of the lithium-adducted conjugates are expected to be even greater but these could not be reliably obtained under these experimental conditions (*see above*). These quantitative rate data show that gas-phase ozonolysis of unsaturated ions is intrinsically slow but, importantly, the reaction efficiency can be increased over two-orders of magnitude by simply changing the identity of the cationizing reagent. These data thus provide important insight into future analytical developments of OzID.

*Selective detection of CLAs*

The utility of OzID as a method for the selective detection and characterization of conjugated lipids was tested on lipid extracts from selected sources. Safflower oil and a dietary supplement were subjected to lipid extraction, hydrolysis, and derivatization using standard procedures. The resulting unfractionated FAMEs were then mixed with sodium acetate solution and infused directly into the ESI source of the QTRAP to facilitate the OzID analysis of $[FAME+Na]^+$ ions. Figures 5(a) and (b) show OzID spectra obtained from sodiated FAME (18:2) ions mass-selected at *m/z* 317 from infusion-ESI of extracts from the safflower oil and dietary supplement, respectively. The spectrum obtained from the safflower extract closely resembles that obtained from authentic FAME (18:2(9*Z*,12*Z*)) (Figure 1c) with the product ions at *m/z* 209 and 249 indicative of double bonds in the *n*-9 and *n*-6 double-bond positions, respectively. OzID provides no evidence for the presence of CLAs in this sample; this finding is supported by independent GC analysis of the same extract from which only FAME (18:2(9*Z*,12*Z*)) and its geometric isomer FAME (18:2(9*E*,12*E*)) were observed (see Figure S1 of Supporting Information). In contrast, OzID on the dietary supplement extract shows evidence for a mixture of conjugated compounds due to the presence of even-*m/z* product ions (marked with an asterisk (*) in Figure 5b). The even-*m/z* ions at *m/z* 248 and 262 are consistent with those previously observed for the conjugated lipids, FAME (18:2(9Z,11E)) and FAME (18:2(10*E*,12*Z*)), respectively (*cf*. Figure 1a and b). Two pairs of aldehyde ions are identified in this spectrum that indicate double bonds in the *n*-7 and *n*-9 positions for one lipid (*i.e.*, *m/z* 235 and 209) and *n*-6

and *n*-8 in the other (*i.e.*, *m/z* 249 and 223). Taken together, these data demonstrate that at least two conjugated linoleic acid isomers are present in the dietary supplement and the double-bond positions in each of these can be uniquely assigned based on the OzID spectrum alone. This conclusion is supported by GC analysis which reveals two prominent peaks corresponding in retention time to authentic FAME (18:2(9Z,11E)) and FAME (18:2(10*E*,12*Z*)) isomers (Figure S1). The comparison of OzID and GC analysis for these extracts is instructive. On the one hand, the OzID spectra in Figure 5 allow the assignment of double-bond position and identify the presence of an isomeric mixture without fractionation or comparison to authentic standards. However, the assignment of double-bond geometry (*i.e.*, *cis* and *trans*) required confirmation by GC, yet this could only be achieved with comparison of retention times to those independently obtained for standard compounds. While chromatographic separation required a 50-min elution time for both extracts and standards, the OzID spectrum for the safflower extract was obtained in under 2 min (using a 2-s reaction time) and the equivalent dietary supplement analysis took less than 2 s (with a 50-ms reaction time). This comparison suggests that OzID combined with direct infusion-ESI approaches can provide a rapid and structurally informative approach to the analysis of FAMEs; however, some form of chromatography may still be required for assignment of double-bond geometries. Future endeavours will focus on combining OzID with liquid-chromatography in order to harness the complementarity of each approach.

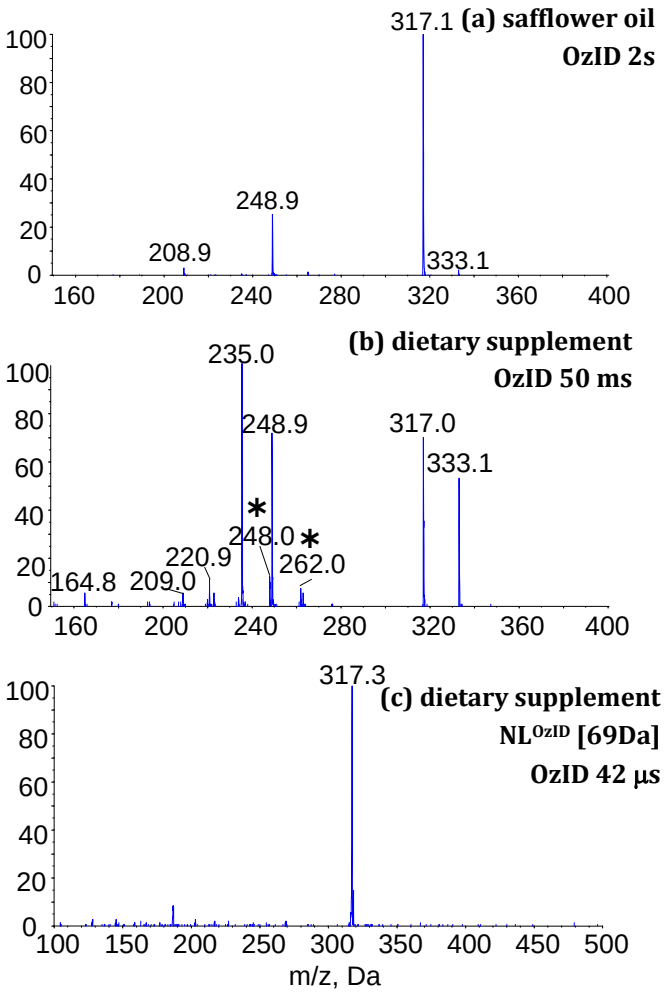


**Figure 5** Spectra acquired on a tandem linear ion-trap mass spectrometer. The top two panels show OzID on $[M+Na]^+$ precursor ions at *m/z* 317 isolated from the ESI of (derivatized) extracts from commercially available samples of (a) safflower oil and (b) CLA dietary supplements. Panel (c) shows a $NL^{OzID}$ scan of -69 Da uniquely identifies the presence of the conjugated FAME (18:2(9*Z*,11*E*)) in the supplements. Reaction times are indicated for each experiment and represent the time ions are isolated in the presence of ozone. The 42-µs reaction time in (c) is based on an estimated transmission time through q2

*OzID without ion trapping*

The significant enhancement in reaction rates measured for conjugated lipids with ozone suggested that it might be possible to carry out OzID analyses by simply passing the selected-ions through the reagent gas (*i.e.*, without trapping the ions, or a beam-type experiment). Conceptually, this presents a number of advantages. First, the majority of contemporary lipidomic analyses are undertaken using triple quadrupole platforms, most of which cannot readily trap mass-selected ions. Second, if the chemistry can be observed on the time-scale of a beam-type experiment, then OzID could be employed with neutral loss and precursor-ion experiments often exploited in lipid mass spectrometry. Cole and Enke have previously demonstrated the principle of applying neutral gain scans based on selective ion-molecule reactions between ethyl vinyl ether and phospholipids for the characterization of phospholipid class [48]. The triple quadrupole geometry of the modified QTRAP mass spectrometer used here is ideal for testing the efficacy of OzID in a beam-type experiment. This was first undertaken by measuring a conventional tandem mass spectrum of *m/z* 317 mass-selected from the dietary supplement extract with ozone present in q2. This spectrum (data not shown) revealed the same diagnostic OzID ions as observed in Figure 5(b), albeit at lower abundance. Following this demonstration, a neutral loss (NL) experiment was performed on the same sample using a constant offset of -69 Da corresponding to the loss of the diagnostic hydrocarbon radical identified in Figure 1(a). The resulting $NL^{OzID}$ spectrum is shown in Figure 5(c) and highlights the selective detection of *m/z* 317 due to the presence of the FAME (18:2(9*Z*,11*E*)) conjugated isomer in this sample. Although preliminary, these data suggest that such an approach could represent a new tool for searching for conjugated fatty acids in complex matrices. Significantly, $NL^{OzID}$ is compatibile with contemporary infusion-ESI approaches to lipidomics analysis on triple quadrupole platforms.

## CONCLUSIONS

This study has uncovered intriguing reactivity trends for OzID analyses of ionized FAME (18:2) isomers in terms of overall reaction rates as well as unique product ions. The ozonolysis rates of a given [FAME (18:2)+X]$^+$ ion, where X is an alkali metal ion, were seen to increase for metal ions of decreasing radius, while geometrical isomers for a given metal showed relative rate increases from *cis*- to *trans*- consistent with those from ozonolysis of neutral gas-phase olefins. More outstandingly, an increase of more than two orders of magnitude is observed for the relative ozonolysis rate constants between non-conjugated and conjugated isomers. This rate enhancement can be exploited to increase the sensitivity of CLA detection in the OzID analyses of mixtures while characteristic odd-mass neutral losses confirm the presence of double-bond conjugation in these systems. The combination of fast reaction kinetics and unique product ions for conjugated carbon-carbon double-bond motifs makes OzID a sensitive and selective technique for CLA detection in mixtures. Moreover, the same approach could be deployed in future searches for the conjugated double-bond motif in intact complex lipids (*i.e.*, phospholipids, triacylglycerols, sphingomyelins *etc.*), thus providing new insights into the carriers of CLAs in biological systems.

The increased reaction rates of OzID for conjugated FAMEs have been exploited in a neutral loss experiment on a triple quadrupole instrument to detect a single conjugated isomer selectively from an unfractionated mixture. This is the first time OzID has been successfully performed as a beam-type experiment (*i.e.,* a non-trapping experiment) and, combined with previously described sensitivity gains in the tandem linear ion-trap geometry [32], suggest an increasing compatibility of OzID with high-throughput methods employed in global lipidomics.

**Acknowledgements:**

S.J.B. and T.W.M. are grateful to the Australian Research Council (ARC) and AB SCIEX for support of this research through the Linkage scheme (LP110200648). H.T.P. is supported by a matching scholarship from the University of Wollongong and the ARC (DP0986628). T.W.M. is an ARC

*Future Fellow* (FT110100249) and S.J.B. is supported by the ARC Centre of Excellence for Free Radical Chemistry and Biotechnology (CE0561607). We acknowledge the contributions of Dr Berwyck Poad (UOW) in the initial modifications to the QTRAP2000 mass spectrometer and thank Dr John Korth (UOW) for assistance with GC-MS analysis.

## References


1. Pestana, J. M., Costa, A. S. H., Martins, S. V., Alfaia, S. P. A., Alves, S. P., Bessa, R. J. B., Prates, J. A. M.: Effect of slaughter season and muscle type on the fatty acid composition, including conjugated linoleic acid isomers, and nutritional value of intramuscular fat in organic beef. *J. Sci. Food Agric.* doi: 10.1002/jsfa.5648 (2012)

2. Pan, X., Wang, X.: Profiling of plant hormones by mass spectrometry. *J. Chromatogr. B* **877**, 2806-2813 (2009)

3. Fang, N. B., Teal, P. E. A., Doolittle, R. E., Tumlinson, J. H.: Biosynthesis of conjugated olefinic systems in the sex-pheromone gland of female tobacco hornworm moths, manduca-sexta (l). *Insect Biochem. Mol. Biol.* **25**, 39-48 (1995)

4. Lienard, M. A., Lassance, J.-M., Wang, H.-L., Zhao, C.-H., Piskur, J., Johansson, T., Lofstedt, C.: Elucidation of the sex-pheromone biosynthesis producing 5,7-dodecadienes in Dendrolimus punctatus (Lepidoptera: Lasiocampidae) reveals Delta 11-and Delta 9-desaturases with unusual catalytic properties. *Insect Biochem. Mol. Biol.* **40**, 440-452 (2010)

5. Pariza, M. W.: Perspective on the safety and effectiveness of conjugated linoleic acid. *Am. J. Clin. Nutr.* **79**, 1132S-1136S (2004)

6. Lee, K., Paek, K., Lee, H. Y., Park, J. H., Lee, Y.: Antiobesity effect of trans-10,cis-12-conjugated linoleic acid-producing Lactobacillus plantarum PL62 on diet-induced obese mice. *J. Appl. Microbiol.* **103**, 1140-1146 (2007)

7. Schmid, A., Collomb, M., Sieber, R., Bee, G.: Conjugated linoleic acid in meat and meat products: A review. *Meat Science* **73**, 29-41 (2006)

8. Fritsche, J., Steinhart, H.: Amounts of conjugated linoleic acid (CLA) in German foods and evaluation of daily intake. *Z. Lebensm. Unters. Forsch. A* **206**, 77-82 (1998)

9. Villeneuve, P., Lago, R., Barouh, N., Barea, B., Piombo, G., Dupre, J. Y., Le Guillou, A., Pina, M.: Production of conjugated linoleic acid isomers by dehydration and isomerization of castor bean oil. *J. Am. Oil Chem. Soc.* **82**, 261-269 (2005)

10. Uehara, H., Suganuma, T., Negishi, S., Ueno, S., Sato, K.: A Novel Method for Solvent Fractionation of Two CLA Isomers. *J. Am. Oil Chem. Soc.* **73**, 261-267 (2006)

11. Gammill, W., Proctor, A., Jain, V.: Comparative Study of High-Linoleic Acid Vegetable Oils for the Production of Conjugated Linoleic Acid. *J. Agric. Food. Chem.* **58**, 2952-2957 (2010)

12. Pariza, M. W., Park, Y., Cook, M. E.: The biologically active isomers of conjugated linoleic acid. *Prog. Lipid Res.* **40**, 283-298 (2001)

13. Evans, M. E., Brown, J. M., McIntosh, M. K.: Isomer-specific effects of conjugated linoleic acid (CLA) on adiposity and lipid metabolism. *J. Nutr. Biochem.* **13**, 508-516 (2002)

14. Loor, J. J., Herbein, J. H.: Reduced fatty acid synthesis and desaturation due to exogenous trans10, cis12-CLA in cows fed oleic or linoleic oil. *J. Dairy Sci.* **86**, (2003)

15. Loor, J. J., Lin, X. B., Herbein, J. H.: Effects of dietary cis 9, trans 11-18 : 2, trans 10, cis 12-18 : 2 or vaccenic acid (trans 11-18 : 1) during lactation on body composition, tissue fatty acid profiles, and litter growth in mice. *Br. J. Nutr.* **90**, (2003)

16. De La Torre, A., Debiton, E., Durand, D., Chardigny, J. M., Berdeaux, O., Loreau, O., Barthomeuf, C., Bauchart, D., Gruffat, D.: Conjugated linoleic acid isomers and their conjugated derivatives inhibit growth of human cancer cell lines. *Anticancer Res.* **25**, (2005)

17. Ringseis, R., Koenig, B., Leuner, B., Schubert, S., Nass, N., Stangl, G., Eder, K.: LDL receptor gene transcription is selectively induced by t10c12-CLA but not by c9t11-CLA in the human hepatoma cell line HepG2. *Biochim. Biophys. Acta* **1761**, 1235-1243 (2006)

18. Arbones-Mainar, J. M., Navarro, M. A., Guzman, M. A., Arnal, C., Surra, J. C., Acin, S., Carnicer, R., Osada, J., Roche, H. M.: Selective effect of conjugated linoleic acid isomers on atherosclerotic lesion development in apolipoprotein E knockout mice. *Atherosclerosis* **189**, 318-327 (2006)

19. Park, Y., Albright, K. J., Storkson, J. M., Liu, W., Cook, M. E., Pariza, M. W.: Changes in body composition in mice during feeding and withdrawal of conjugated linoleic acid. *Lipids* **34**, 243-248 (1999)

20. Martin, J. C., Gregoire, S., Siess, M. H., Genty, M., Chardigny, J. M., Berdeaux, O., Juaneda, P., Sebedio, J. L.: Effects of conjugated linoleic acid isomers on lipid-metabolizing enzymes in male rats. *Lipids* **35**, 91-98 (2000)

21. Odegaard, A. O., Pereira, M. A.: Trans fatty acids, insulin resistance, and type 2 diabetes. *Nutr. Rev.* **64**, 364-372 (2006)

22. Mitchell, T. W., Pham, H., Thomas, M. C., Blanksby, S. J.: Identification of double bond position in lipids: From GC to OzID. *J. Chromatogr. B* **877**, 2722-2735 (2009)

23. Ståhlman, M., Pham, H., Adiels, M., Mitchell, T., Blanksby, S., Fagerberg, B., Ekroos, K., Borén, J.: Clinical dyslipidaemia is associated with changes in the lipid composition and inflammatory properties of apolipoprotein-B-containing lipoproteins from women with type 2 diabetes. *Diabetologia* **55**, 1156-1166 (2012)

24. Kramer, J. K. G., Cruz-Hernandez, C., Zhou, J.: Conjugated linoleic acids and octadecenoic acids: Analysis by GC. *Eur. J. Lipid Sci. Technol.* **103**, 600-609 (2001)

25. Yurawecz, M. P., Morehouse, K. M.: Silver-ion HPLC of conjugated linoleic acid isomers. *Eur. J. Lipid Sci. Technol.* **103**, 609-613 (2001)

26. Park, Y., Storkson, J. M., Albright, K. J., Liu, W., Pariza, M. W.: Biological activities of conjugated fatty acids: conjugated eicosadienoic (conj. 20:2Δc11,t13/t12,c14), eicosatrienoic (conj. 20:3Δc8,t12,c14), and heneicosadienoic (conj. 21:2Δc12,t14/c13,t15) acids and other metabolites of conjugated linoleic acid. *Biochim. Biophys. Acta* **1687**, 120-129 (2005)

27. Marques, F. A., Millar, J. G., McElfresh, J. S.: Efficient method to locate double bond positions in conjugated trienes. *J. Chromatogr. A* **1048**, 59-65 (2004)

28. Xu, Y., Brenna, J. T.: Atmospheric pressure covalent adduct chemical ionization tandem mass spectrometry for double bond localization in monoene- and diene-containing triacylglycerols. *Anal. Chem.* **79**, 2525-2536 (2007)

29. Michaud, A. L., Yurawecz, M. P., Delmonte, P., Corl, B. A., Bauman, D. E., Brenna, J. T.: Identification and characterization of conjugated fatty acid methyl esters of mixed double bond geometry by acetonitrile chemical ionization tandem mass spectrometry. *Anal. Chem.* **75**, 4925-4930 (2003)

30. Thomas, M. C., Mitchell, T. W., Harman, D. G., Deeley, J. M., Nealon, J. R., Blanksby, S. J.: Ozone-induced dissociation: Elucidation of double bond position within mass-selected lipid ions. *Anal. Chem.* **80**, 303-311 (2008)

31. Deeley, J. M., Thomas, M. C., Truscott, R. J. W., Mitchell, T. W., Blanksby, S. J.: Identification of abundant alkyl ether glycerophospholipids in the human lens by tandem mass spectrometry techniques. *Anal. Chem.* **81**, 1920-1930 (2009)

32. Poad, B. L. J., Pham, H. T., Thomas, M. C., Nealon, J. R., Campbell, J. L., Mitchell, T. W., Blanksby, S. J.: Ozone-Induced Dissociation on a Modified Tandem Linear Ion-Trap: Observations of Different Reactivity for Isomeric Lipids. *J. Am. Soc. Mass. Spectrom.* **21**, 1989-1999 (2010)

33. Fahy, E., Subramaniam, S., Brown, H. A., Glass, C. K., Merrill, A. H., Murphy, R. C., Raetz, C. R. H., Russell, D. W., Seyama, Y., Shaw, W., Shimizu, T., Spener, F., van Meer, G., VanNieuwenhze, M. S., White, S. H., Witztum, J. L., Dennis, E. A.: A comprehensive classification system for lipids. *J. Lipid Res.* **46**, 839-861 (2005)

34. Fahy, E., Subramaniam, S., Murphy, R. C., Nishijima, M., Raetz, C. R. H., Shimizu, T., Spener, F., van Meer, G., Wakelam, M. J. O., Dennis, E. A.: Update of the LIPID MAPS comprehensive classification system for lipids. *J. Lipid Res.* **50**, S9-S14 (2009)

35. The nomenclature of lipids (recommendations 1976). IUPAC-IUB Commission on Biochemical Nomenclature. *J. Lipid Res.* **19**, (1978)

36. Brown, S. H. J., Mitchell, T. W., Blanksby, S. J.: Analysis of unsaturated lipids by ozone-induced dissociation. *Biochim. Biophys. Acta* **1811**, 807-817 (2011)

37. Dobson, G., Christie, W. W.: Mass spectrometry of fatty acid derivatives. *Eur. J. Lipid Sci. Technol.* **104**, 36-43 (2002)

38. Ran-Ressler, R. R., Lawrence, P., Brenna, J. T.: Structural characterization of saturated branched chain fatty acid methyl esters by collisional dissociation of molecular ions generated by electron ionization. *J. Lipid Res.* **53**, 195-203 (2012)

39. Henry, D. J., Parkinson, C. J., Mayer, P. M., Radom, L.: Bond dissociation energies and radical stabilization energies associated with substituted methyl radicals. *J. Phys. Chem. A* **105**, 6750-6756 (2001)

40. Pryor, W. A.: Mechanisms of radical formation from reactions of ozone with target molecules in the lung. *Free Radical Biol. Med.* **17**, 451-465 (1994)

41. Treacy, J., Elhag, M., Ofarrell, D., Sidebottom, H.: Reactions of ozone with unsaturated organic compounds. *Ber. Bunsenges. Phys. Chem.* **96**, 422-427 (1992)

42. Lewin, A. G., Johnson, D., Price, D. W., Marston, G.: Aspects of the kinetics and mechanism of the gas-phase reactions of ozone with conjugated dienes. *PCCP* **3**, 1253-1261 (2001)

43. Avzianova, E. V., Ariya, P. A.: Temperature-Dependent Kinetic Study for Ozonolysis of Selected Tropospheric Alkenes. *Int. J. Chem. Kinet.* **34**, 678-684 (2002)

44. Rodgers, M. T., Armentrout, P. B.: Noncovalent metal-ligand bond energies as studied by threshold collision-induced dissociation. *Mass Spectrom. Rev.* **19**, 215-247 (2000)

45. Premkumar, J. R., Vijay, D., Sastry, G. N.: The significance of the alkene size and the nature of the metal ion in metal-alkene complexes: a theoretical study. *Dalton Trans.* **41**, 4965-4975 (2012)

46. Williams, S., Campos, M. F., Midey, A. J., Arnold, S. T., Morris, R. A., Viggiano, A. A.: Negative ion chemistry of ozone in the gas phase. *J. Phys. Chem. A* **106**, 997-1003 (2002)

47. Su, T., Chesnavich, W. J.: Parametrization of the ion-polar molecule collision rate constant by trajectory calculations. *J. Chem. Phys.* **76**, 5183-5185 (1982)

48. Cole, M. J., Enke, C. G.: Fast-atom-bombardment tandem mass spectrometry employing ion-molecule reactions for the differentiation of phospholipid classes. *J. Am. Soc. Mass. Spectrom.* **2**, 470-475 (1991)

**Figures, Schemes, and Tables**

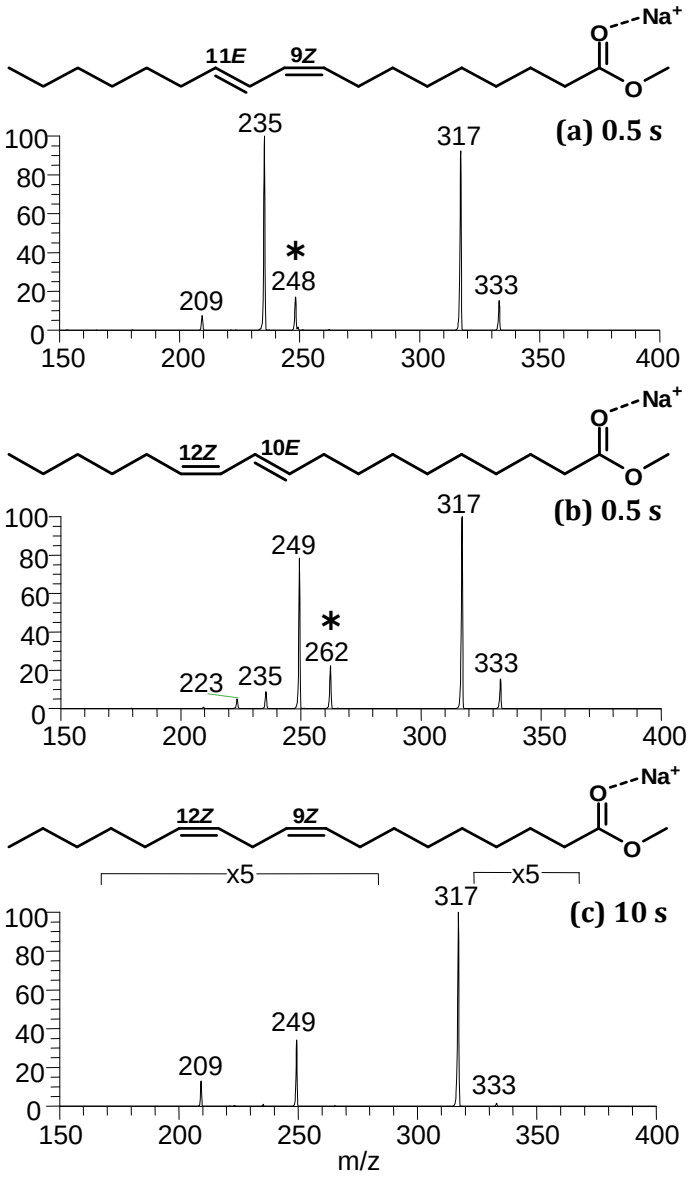


**Figure 1** OzID spectra acquired for sodium adducts of three FAME (18:2) isomers (a) conjugated [FAME (18:2(9*Z*,11*E*))+Na]$^+$ for a 0.5 s reaction time, (b) conjugated [FAME (18:2(10*E*,12*Z*))+Na]$^+$ for a 0.5 s reaction time and (c) non-conjugated [FAME (18:2(9*Z*,12*Z*))+Na]$^+$ for a 10 s reaction time. [M+Na]$^+$ precursor ions appear at *m/z* 317 in all three spectra, as well as an [M+Na+16]$^+$ ion at *m/z* 333. Peaks with an even *m/z* correspond to radical cations formed from conjugated FAMEs and are marked with an asterisk (∗)

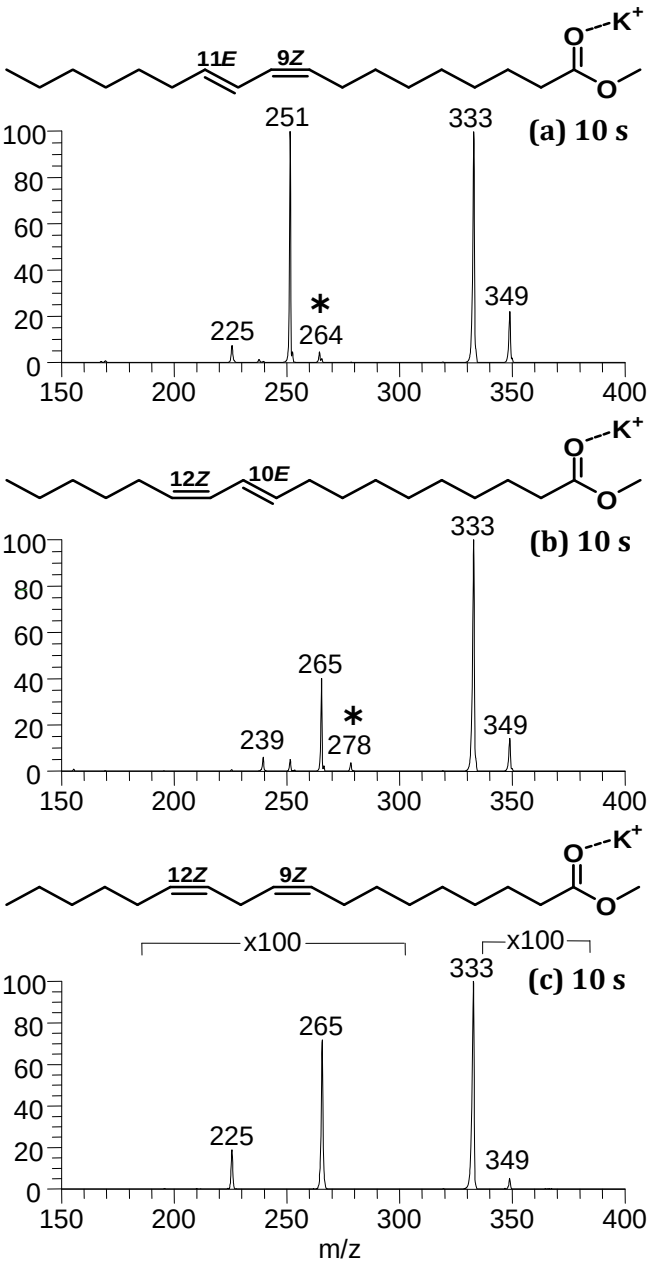


**Figure 2** OzID spectra acquired with a 10 s reaction time in each case for potassium adducts of the FAME (18:2) isomer precursor ions at *m/z* 333: (a) conjugated [FAME (18:2(9*Z*,11*E*))+K]$^+$, (b) conjugated [FAME (18:2(10*E*,12*Z*))+K]$^+$ and (c) non-conjugated [FAME (18:2(9*Z*,12*Z*))+K]$^+$. Peaks with an even mass correspond to radical cations formed from conjugated FAMEs and are marked with an asterisk (∗)

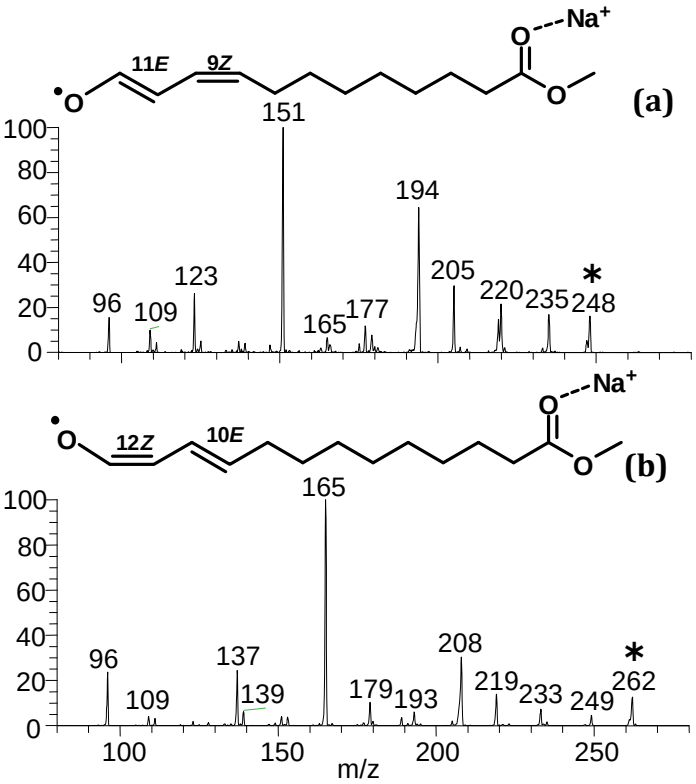


**Figure 3** OzID/CID spectra obtained by performing CID on the even-mass OzID ions derived from the conjugated isomers (a) [FAME(18:2 (9*Z*,11*E*))+Na]$^+$ and (b) [FAME(18:2 (10*E*,12*Z*))+Na]$^+$. The proposed structures of the radical cations at *m/z* 248 and 262 ions are drawn above each spectrum

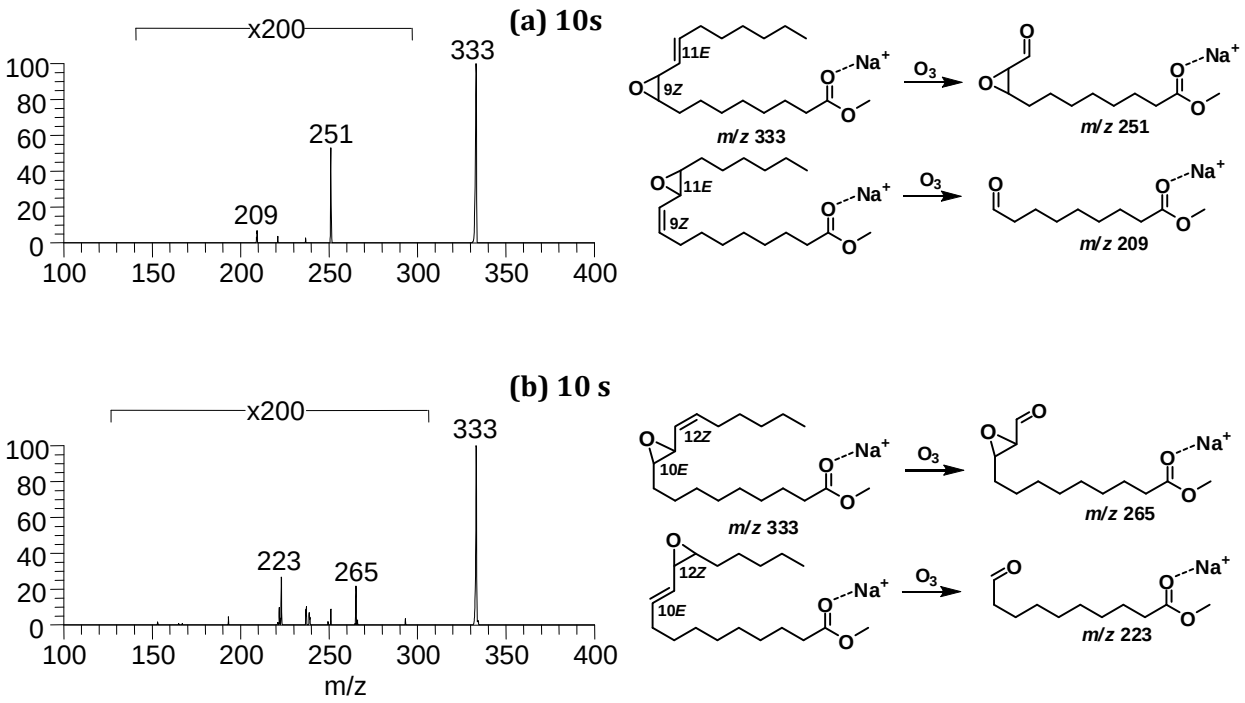


**Figure 4** OzID/OzID spectra acquired with a 10 s reaction time in each case for the $[M+Na+16]^+$ ions derived from OzID of the two conjugated FAME (18:2) isomers (a) FAME (18:2(9*Z*,11*E*)) and (b) FAME (18:2(10*E*,12*Z*)). The two major product ions marked in each spectrum can be rationalized as aldehydes formed from the OzID of the putative epoxide structures shown

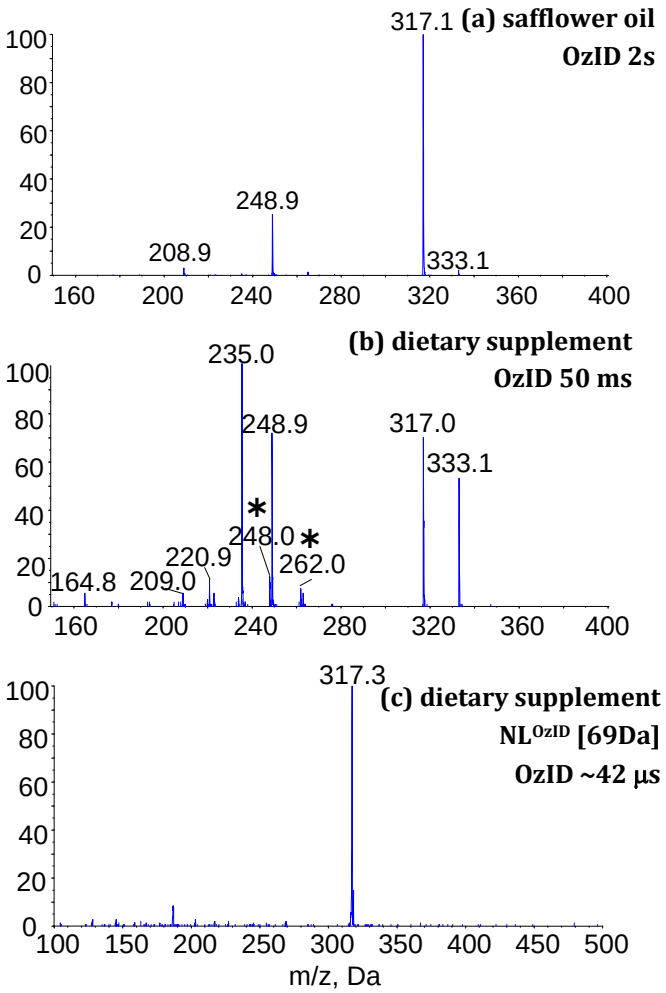


**Figure 5** Spectra acquired on a tandem linear ion-trap mass spectrometer. The top two panels show OzID on $[M+Na]^+$ precursor ions at *m/z* 317 isolated from the ESI of (derivatized) extracts from commercially available samples of (a) safflower oil and (b) CLA dietary supplements. Panel (c) shows a $NL^{OzID}$ scan of -69 Da uniquely identifies the presence of the conjugated FAME (18:2(9*Z*,11*E*)) in the supplements. Reaction times are indicated for each experiment and represent the time ions are isolated in the presence of ozone. The ~42-µs reaction time in (c) is based on an estimated transmission time through q2

**Scheme I** Proposed reaction pathways for OzID on the sodium adducts of (a) the conjugated FAME (18:2(9*Z*,11*E*)) and (b) the non-conjugated FAME (18:2(9*Z*,12*Z*)). The two aldehyde product ions in each case can be used to locate the positions of unsaturation for each isomer unambiguously

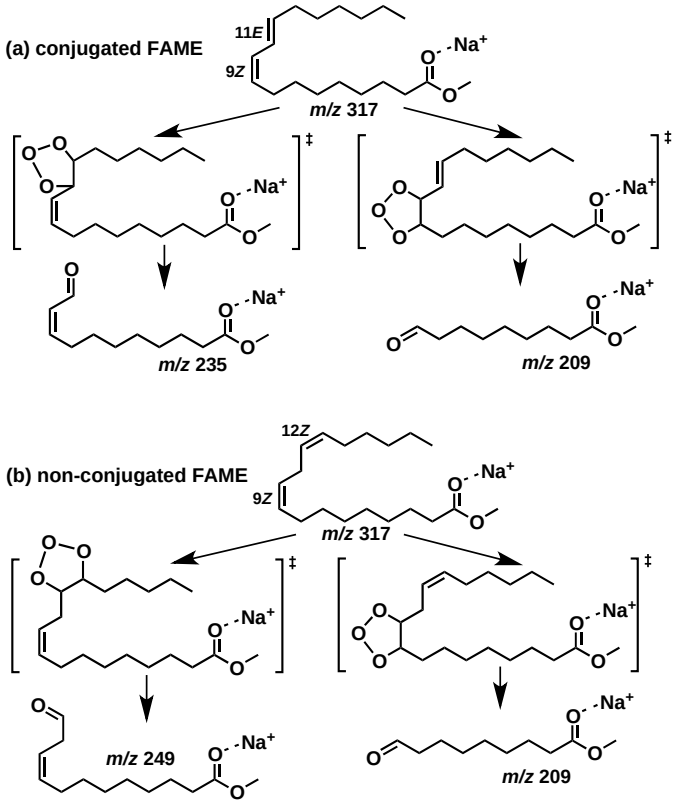

**Scheme II** Proposed mechanism for the formation of the radical cation (*m/z* 248) upon OzID of the conjugated [FAME (18:2(9*Z*,11*E*))+Na]$^+$

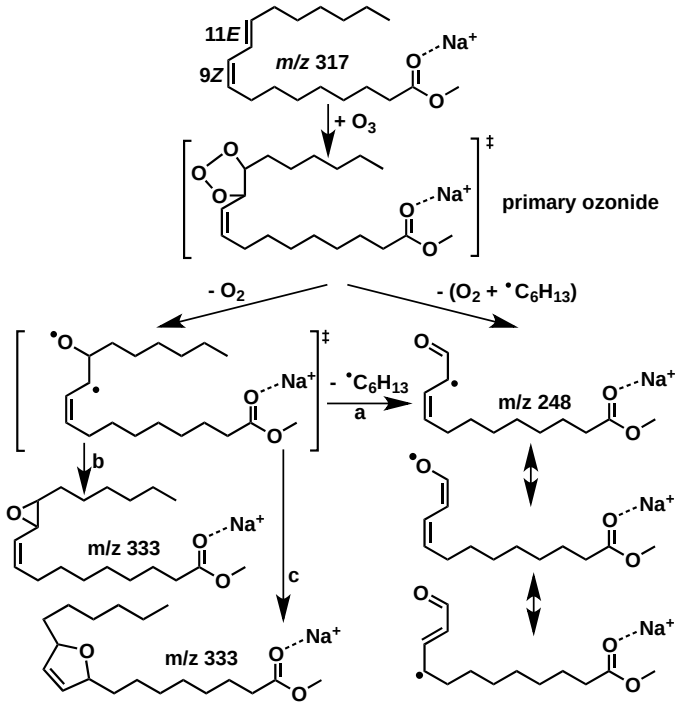

**Table 1** Rate constants measured on a tandem linear ion-trap mass spectrometer (QTRAP) for the gas-phase ozonolysis reactions of metal adducted FAME standards. Pseudo-first-order values, $k^{I}$, were calculated from raw kinetics data provided as Supporting Information (Figure S4). The absolute second order rate constants, $k^{II}$, are calculated by benchmarking to the known $k^{II}$ for the gas-phase reaction $I^- + O_3 \rightarrow IO_3^-$ [46]. Reaction efficiencies ($\Phi$) are presented in square brackets as a percentage of the calculated collision rate.

| | $k^{I} = k^{II}[O_3]$ $(s^{-1})$[f] | | | | $k^{II}$ $(x10^{-12}$ $cm^3$ $molecules^{-1}$ $s^{-1})$ $[\Phi\ \%]$[a] | |
|---|---|---|---|---|---|---|
| Metal adduct **FAME (18:2)** | $K^+$ | $Na^+$ | $Li^+$ | | $K^+$ | $Na^+$ | $Li^+$ |
| **(9*Z*,11*E*)** | 3.20 ± 0.02 | 1.30 ± 0.05[e] | -[d] | | 4 ± 1 [0.5] | 110 ± 30 [14][e] | -[d] |
| **(10*E*,12*Z*)** | 1.60 ± 0.02 | 17.6 ± 0.3 | -[d] | | 2.1 ± 0.5 [0.3] | 23 ± 6 [3] | -[d] |
| **(9*Z*,12*Z*)** | 0.0411 ± 0.0006 | 0.357 ± 0.003 | 5.50 ± 0.03 | | 0.05 ± 0.01 [0.01] | 0.5 ± 0.1 [0.1] | 7 ± 2 [0.9] |
| **(9*E*,12*E*)** | 0.064 ± 0.001 | 0.503 ± 0.003 | 7.7 ± 0.1 | | 0.08 ± 0.02 [0.01] | 0.6 ± 0.2 [0.1] | 10 ± 2 [1] |
| $I^-$ | 7.8 ± 0.1[b] | | | | 10 ± 3[c] | | |

a. Reaction efficiencies based on theoretical collision rates calculated from a parameterized trajectory model [47].
b. $I^-$ was run before and after all FAME experiments were conducted to monitor ozone concentration.
c. Reference [46].
d. Reactions were too fast for reliable measurements under these experimental conditions.
e. $[FAME(18:2\ (9Z,11E))+Na]^+$ was run on a separate day under ozone conditions which yielded $k^{I}(I^-) = 0.122 \pm 0.003\ s^{-1}$.
f. Errors in $k^{I}$ values represent the standard error in the slope of a line fit to the data (see Supporting Information Figure S4); errors in $k^{II}$ values represent a least squares analysis using the $k^{I}$ errors and the absolute errors of ± 25% quoted by Williams *et al.* [46].